

# Hydroperoxide-Mediated Degradation of Acetonitrile in the Lithium–Air Battery

Rory C. McNulty, Kieran D. Jones, Conrad Holc, Jack W. Jordan, Peter G. Bruce, Darren A. Walsh, Graham N. Newton, Hon Wai Lam, and Lee R. Johnson\*

Understanding and eliminating degradation of the electrolyte solution is arguably the major challenge in the development of high energy density lithium–air batteries. The use of acetonitrile provides cycle stability comparable to current state-of-the-art glyme ethers and, while solvent degradation has been extensively studied, no mechanism for acetonitrile degradation has been proposed. Through the application of in situ pressure measurements and ex situ characterization to monitor the degradation of acetonitrile in the lithium–air battery, a correlation between H<sub>2</sub>O concentration within the cell and deviation from the idealized electron/oxygen ratio is revealed. Characterization of the cycled electrolyte solution identifies acetamide as the major degradation product under both cell and model conditions. A new degradation pathway is proposed that rationalizes the formation of acetamide, identifies the role of H<sub>2</sub>O in the degradation process, and confirms lithium hydroperoxide as a critical antagonistic species in lithium–air cells for the first time. These studies highlight the importance of considering the impact of atmospheric gases when exploring lithium–air cell chemistry and suggest that further exploration of the impact of hydroperoxide species on the degradation in lithium–air cells may lead to identification of more effective electrolyte solvents.

O<sub>2</sub> on the surface of a lightweight porous carbon positive electrode to form Li<sub>2</sub>O<sub>2</sub>. On charge, the reaction is reversed. The chemistry and performance of the battery is heavily influenced by the nature of the electrolyte solution, which can control the mechanism of the O<sub>2</sub> reduction reaction and is also known to undergo significant degradation.<sup>[4,7–9]</sup> Consequently, the practical performance and cycle life of the battery is largely dictated by the electrolyte composition, and identifying a practical, stable solvent is perhaps the biggest factor limiting cell development.<sup>[7,9]</sup>

Extensive efforts have been made to understand electrolyte solution degradation mechanisms, and several antagonistic intermediates including lithium superoxide (LiO<sub>2</sub>),<sup>[10,11]</sup> lithium peroxide (Li<sub>2</sub>O<sub>2</sub>),<sup>[12]</sup> polyoxides,<sup>[13,14]</sup> and singlet oxygen (<sup>1</sup>O<sub>2</sub>)<sup>[15]</sup> have been identified.<sup>[16,17]</sup> However, their specific roles remain an area of active debate. Early Li–air cells contained organic carbonates and dimethyl sulfoxide,<sup>[18–21]</sup>

but these were susceptible to degradation by LiO<sub>2</sub> formed during discharge.<sup>[22–24]</sup> Amide- and sulfone-containing solvents were similarly shown to undergo oxidative degradation.<sup>[25–27]</sup> Glyme ether solvents are widely used due to their oxidative robustness; however, they are proposed to undergo deprotonation with LiO<sub>2</sub>

## 1. Introduction

The lithium–air (Li–air) battery has one of the highest theoretical specific energies (3495 Wh kg<sup>−1</sup>) of any next-generation battery chemistry, making it ideal for weight-sensitive applications.<sup>[1–6]</sup> The battery operates through the reduction of

R. C. McNulty, K. D. Jones, C. Holc, J. W. Jordan, D. A. Walsh, G. N. Newton, L. R. Johnson  
Nottingham Applied Materials and Interfaces Group  
School of Chemistry  
University of Nottingham  
Nottingham NG7 2TU, UK  
E-mail: lee.johnson@nottingham.ac.uk

 The ORCID identification number(s) for the author(s) of this article can be found under <https://doi.org/10.1002/aenm.202300579>

© 2023 The Authors. Advanced Energy Materials published by Wiley-VCH GmbH. This is an open access article under the terms of the Creative Commons Attribution License, which permits use, distribution and reproduction in any medium, provided the original work is properly cited.

DOI: 10.1002/aenm.202300579

R. C. McNulty, C. Holc, J. W. Jordan, P. G. Bruce, D. A. Walsh, G. N. Newton, L. R. Johnson  
The Faraday Institution  
Quad One  
Harwell Science and Innovation Campus  
Didcot OX11 0RA, UK  
R. C. McNulty, K. D. Jones, C. Holc, J. W. Jordan, D. A. Walsh, G. N. Newton, H. W. Lam, L. R. Johnson  
School of Chemistry  
University of Nottingham  
Nottingham NG7 2TU, UK  
P. G. Bruce  
Department of Materials and Chemistry  
University of Oxford  
Parks Road, Oxford OX1 3PH, UK

and/or  $\text{Li}_2\text{O}_2$ ,<sup>[28,29]</sup> and exhibit  $\text{Li}_2\text{O}_2$  discharge yields of no more than 95%.<sup>[30,31]</sup> Early studies showed that acetonitrile (MeCN) is stable toward  $\text{Li}_2\text{O}_2$  with a relatively high activation barrier for nucleophilic attack and deprotonation by  $\text{O}_2^-$ .<sup>[32–34]</sup> The oxygen solubility and diffusivity in MeCN is similar to those in glyme ethers, and its dielectric constant results in high electrolyte conductivities.<sup>[35]</sup> While the vapor pressure of MeCN is high, it is similar to that of commonly used dimethoxyethane, and higher molecule weight nitriles with negligible vapor pressure have been reported for use in batteries.<sup>[36–39]</sup> Despite this, the capacity of cells containing MeCN electrolytes is limited by poor  $\text{LiO}_2$  solubility, which results in surface passivation at the positive electrode. However, the use of redox mediators, which are routinely employed to facilitate solution-phase catalytic  $\text{O}_2$  reduction,<sup>[40,41]</sup> has made the requirement of high  $\text{LiO}_2$  solubility redundant.<sup>[30,42]</sup> Some recent studies have shown that MeCN-based cells can support significantly higher capacities than initially reported.<sup>[43,44]</sup> As studies in this area are limited, further investigation of MeCN as a potential Li–air electrolyte solvent is needed.

The promise of MeCN as an electrolyte solvent is supported by Luntz and co-workers who identified MeCN as having an  $e^-/\text{O}_2$  yield of 2.05, similar to glyme ethers, and the highest oxygen reduction/oxygen evolution reaction efficiency ( $\approx 0.9$ ) of solvents explored.<sup>[45,46]</sup> While promising, these results indicate that MeCN suffers from degradation reactions that are yet to be identified. As with the vast majority of Li–air battery research, degradation studies typically involve the use of pure  $\text{O}_2$  gas streams only.<sup>[3,47]</sup> However, a practical battery will either use an atmospheric air stream, containing  $\text{H}_2\text{O}$  and  $\text{CO}_2$ , or require signifi-

cant air purification systems, which limit the gravimetric impact of the technology.<sup>[47]</sup>  $\text{H}_2\text{O}$  has been shown to trigger the formation of soluble lithium hydroperoxide ( $\text{LiOOH}$ ) in the cell, which can increase capacity.<sup>[48–52]</sup> The introduction of  $\text{H}_2\text{O}$  can also result in  $4e^-/\text{O}_2$  reduction to form  $\text{LiOH}$ , particularly in the presence of a catalyst such as iodine, which can increase the capacity, but is also challenging to oxidize.<sup>[53–55]</sup> Critically, these contaminants from the atmosphere may introduce antagonistic intermediates and degradation pathways that lead to cell breakdown, which must be identified and eliminated to achieve a practical Li–air battery.

Herein, we present an analysis of the stability of Li–air cells containing a MeCN-based electrolyte. We show that at high current densities ( $250 \mu\text{A cm}^{-2}$ ), cells containing MeCN exhibit performance comparable to those containing glyme ethers. However, at a lower current density ( $50 \mu\text{A cm}^{-2}$ ), deviation from the ideal  $2e^-/\text{O}_2$  ratio is observed. We identify a relationship between  $\text{H}_2\text{O}$  concentration and  $e^-/\text{O}_2$ , which indicates that  $\text{H}_2\text{O}$ -mediated MeCN degradation occurs. Model chemical systems are employed to replicate conditions within the cell, and acetamide is identified as a degradation product. A reaction mechanism is proposed to account for the electrolyte degradation, which identifies  $\text{LiOOH}$  as a critical antagonistic species in Li–air cells for the first time.

## 2. Results and Discussion

The ideal Li–air electrochemical reaction consumes  $2e^-/\text{O}_2$  on discharge and parasitic (electro)chemical reactions can be identified by any deviation from this ratio. **Figure 1a** shows that

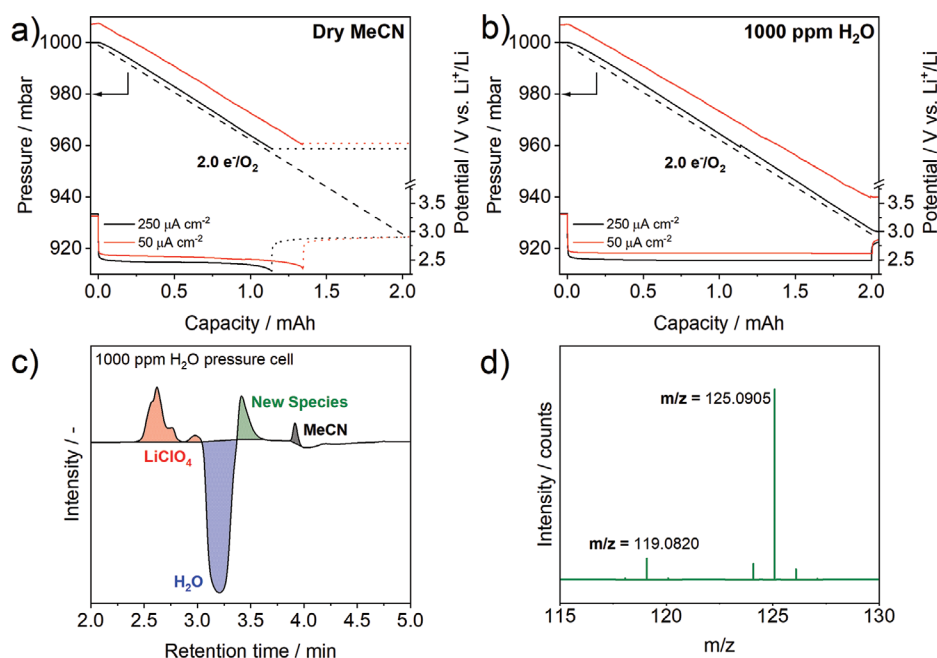


**Figure 1.** a, b) Pressure decay measurements during the first electrochemical discharge of cells containing 0.25 M  $\text{LiClO}_4$  in MeCN at a rate of  $250 \mu\text{A cm}^{-2}$  (black lines) or  $50 \mu\text{A cm}^{-2}$  (red lines) with a) dry electrolyte or b) electrolyte doped with 1000 ppm  $\text{H}_2\text{O}$  compared to the ideal  $2.0 e^-/\text{O}_2$  (black dashed line) pressure decay gradient. The dotted back line indicates the cell open-circuit voltage after reaching the potential limit. c) HPLC chromatogram of a solution made up by soaking the cathode and separator extracted from a pressure cell that was discharged to a capacity of 14.7 mAh with a 0.25 M  $\text{LiClO}_4$  in MeCN doped with 1000 ppm  $\text{H}_2\text{O}$  electrolyte. d) Mass spectrum recorded for the newly identified species at a retention time of 3.5 min.

anhydrous MeCN cells discharged at  $250 \mu\text{A cm}^{-2}$  have an average  $e^-/\text{O}_2$  ratio of 2.04, consistent with previous reports.<sup>[45]</sup> Post-cycling analysis of the positive electrode gave a  $\text{Li}_2\text{O}_2$  yield of 89.6%, comparable to that obtained with state-of-the-art Li–air cells containing glyme ethers.<sup>[30,31]</sup> Unlike at high rates, the analogous cell discharged at  $50 \mu\text{A cm}^{-2}$  did not follow the ideal  $2e^-$  pressure decay gradient, with an  $e^-/\text{O}_2$  ratio of 2.14 (Figure 1a). Higher rates are often used to showcase the performance of a cell; however, the rapid discharge clearly masks degradation pathways that are only evident during long-term cycling. Noting that the cells may contain adventitious  $\text{H}_2\text{O}$ , the electrolyte was extracted from assembled cells and found to contain  $\approx 151$  ppm  $\text{H}_2\text{O}$ . Cells were doped with 1000 ppm of  $\text{H}_2\text{O}$  to understand its influence on the  $e^-/\text{O}_2$  ratio (Figure 1b). At the higher discharge rate of  $250 \mu\text{A cm}^{-2}$ , the  $e^-/\text{O}_2$  ratio was similar to the “dry” cell (2.04  $e^-/\text{O}_2$ ), but at the lower rate of  $50 \mu\text{A cm}^{-2}$ , the ratio deviated to 2.24. This confirms the presence of additional side reactions during discharge. Cells cycled at  $50 \mu\text{A cm}^{-2}$  with  $\text{H}_2\text{O}$  concentrations of 1000, 5000, and 10 000 ppm gave  $e^-/\text{O}_2$  ratios of 2.24, 2.37, and 2.38, respectively, confirming that increasing the  $\text{H}_2\text{O}$  concentration leads to higher levels of parasitic side reactions. To identify soluble degradation products within the cell, high-performance liquid chromatography mass spectrometry (HPLC-MS) was conducted on electrolyte extracted from the cell containing 1000 ppm  $\text{H}_2\text{O}$  discharged to a capacity of 14.7 mAh (Figure 1c; Figure S1, Supporting Information). A new peak was observed with a retention time of 3.42 min, for which mass spectrometry presented signals at 119.1 and 125.1 m/z, which were not observed in the pristine electrolyte (Figure 1d).

To identify the product and elucidate the degradation pathway, a model chemical system was used to mimic the conditions of the electrochemical cell. A heterogeneous mixture containing the mass equivalent ratio of 2 mAh of  $\text{Li}_2\text{O}_2$  in  $d_3$ -MeCN was doped with 1000 ppm  $\text{H}_2\text{O}$ . This solution was used directly for NMR measurements. Figure 2a shows the loss in intensity of the  $\text{H}_2\text{O}$  peak (at 2.165 ppm) in the  $^1\text{H}$  NMR spectrum over 24 h, demonstrating that  $\text{H}_2\text{O}$  reacts in the model system without an applied bias. The reaction mixture was analyzed after 72 h by HPLC-MS, which showed two primary mass peaks at 119.1 and 122.1 m/z (Figure 2b), similar to the species identified in the cell. The difference of 3 Da between these two peaks indicated they are the result of a combination of deuterated ( $\text{CD}_3$ ) and nondeuterated ( $\text{CH}_3$ ) molecular species from reaction with  $d_3$ -MeCN. When repeating the experiment with 20 000 ppm  $\text{H}_2\text{O}$ , a shift in the  $\text{H}_2\text{O}$  peak was observed from 2.53 to 2.51 ppm over 72 h, combined with a slight broadening and decrease in intensity. This indicates a change in the  $\text{H}_2\text{O}$  concentration over the timescale of the measurements (Figure S2, Supporting Information). After 1 h of mixing,  $^1\text{H}$  NMR analysis shows the emergence of two broad singlets at 5.74 and 6.35 ppm, indicative of an amide ( $\text{NH}_2$ ) signal, with the intensity of this signal increasing over the timescale of the experiment (Figure 2c). The  $^{13}\text{C}$  NMR spectrum of the sample after 72 h showed a singlet at 173.8 ppm, consistent with the  $\text{C}=\text{O}$  carbon of  $\text{CD}_3\text{CONH}_2$ , and a quintet at 21.6 ppm, assigned to the methyl carbon of  $\text{CD}_3\text{CONH}_2$  (Figure 2d). HPLC-MS analysis of the sample after 72 h showed three primary mass peaks at 119.1, 122.1, and 125.1 m/z (Figure 2e), and three low intensity peaks at 60.0, 63.1, and 85.0 m/z (Figure 2f). These spectroscopic data confirm the identity of the major

degradation product as acetamide, formed through hydrolysis of MeCN. We note that the primary mass peaks reported are a result of amide dimers, which have been reported previously as the major species in the mass spectrum of acetamide.<sup>[56]</sup> The dominant mass peak in the HPLC-MS of the electrolyte extracted from the discharge cell differs from the chemical system due to the availability of lithium ions from  $\text{LiClO}_4$  producing a lithium adduct,  $[(\text{CH}_3\text{CONH}_2)_2 + \text{Li}]^+$ , 125.1 m/z, as the main product, rather than a hydrogen adduct  $[(\text{CH}_3\text{CONH}_2)_2 + \text{H}]^+$ , 119.1 m/z.

The identification of acetamide in both the model system and electrochemical cell confirms MeCN hydrolysis under discharge conditions. Previous computational work has proposed the Lewis acid-activation of nitrile functional groups occurs when associated with a  $\text{Li}_2\text{O}_2$  surface or solvated lithium cations but suggest that degradation of aliphatic nitriles from peroxide nucleophilic addition is unlikely, due to the poor solubility of reactive lithium peroxide species in MeCN.<sup>[57,58]</sup> However, these studies were limited to anhydrous systems and did not consider practical Li–air cells containing trace atmospheric gases. As discussed above, in the presence of  $\text{H}_2\text{O}$ ,  $\text{LiOOH}$  is known to be in equilibrium with  $\text{Li}_2\text{O}_2$  (Figure 3a).<sup>[48,49]</sup> This equilibrium present in humid Li–air cells mirrors the in situ alkaline hydroperoxide conditions reported for the conversion of nitriles to amides in organic solvents (Figure 3b).<sup>[59–65]</sup>

Our data, specifically the correlation of  $e^-/\text{O}_2$  with  $\text{H}_2\text{O}$  concentration, are consistent with the nucleophilic addition of hydroperoxide to MeCN as a degradation mechanism in Li–air cell chemistry. While a mechanism for hydroperoxide-mediated nitrile hydrolysis is established,<sup>[59–65]</sup> it has not been considered within Li–air batteries. Our proposed MeCN degradation pathway, presented in Figure 4, features  $\text{Li}_2\text{O}_2$  surface-mediated nitrile activation consistent with computation and near ambient pressure X-ray photoemission spectroscopy studies, although solvated lithium cations can also be considered.<sup>[66]</sup> MeCN adsorption to the  $\text{Li}_2\text{O}_2$  surface activates the  $sp$ -hybridized carbon,<sup>[57,58]</sup> facilitating nucleophilic addition of hydroperoxide resulting in the intermediate 1. Protonation of 1 with  $\text{H}_2\text{O}$  gives the imidoperoxoic acid 2, which desorbs from the surface before subsequent reaction with hydroperoxide that give acetamide (3),  $\text{H}_2\text{O}$  and  $\text{O}_2$ .<sup>[60,64,65]</sup>

We note that this  $\text{O}_2$  release would result in an increase in the observed  $e^-/\text{O}_2$  ratio, consistent with our observations during discharge (Figure 1a,b). Although this reaction would eventually consume trace  $\text{H}_2\text{O}$  in the electrolyte, if a gas stream was not subjected to strict purification measures, as discussed by Gallagher et al.,<sup>[47]</sup> continual replenishment of  $\text{H}_2\text{O}$  would result in the unabating hydrolysis of MeCN. Furthermore, it is important to note that hydroperoxide-mediated degradation may not be exclusive to MeCN and could be active in other electrolyte compositions containing cyano groups or other electrophilic functionalities.

### 3. Conclusions

We have identified a new degradation pathway for MeCN by a soluble antagonistic intermediate species,  $\text{LiOOH}$ , that will inevitably be present in a practical Li–air battery. The same chemical equilibria that are known to facilitate  $\text{H}_2\text{O}$ -mediated phase transfer catalysis of  $\text{Li}_2\text{O}_2$  with trace quantities of  $\text{H}_2\text{O}$  also represent reaction conditions for the hydrolysis of nitriles used in

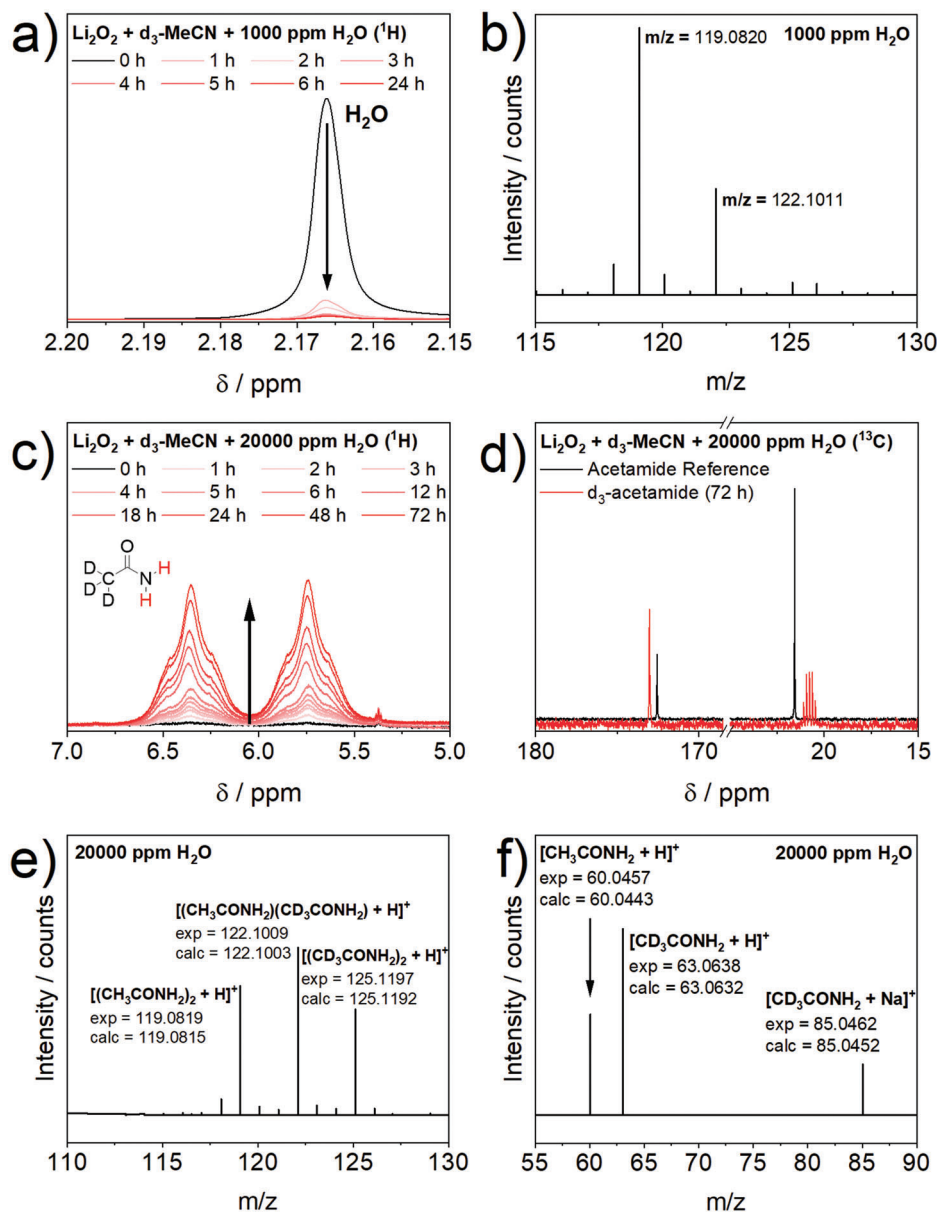
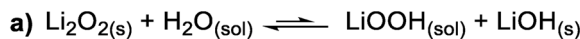


**Figure 2.** Spectroscopic analysis of an aliquot from a heterogeneous mixture of  $\text{Li}_2\text{O}_2$  in  $\text{d}_3\text{-MeCN}$  with either a,b) 1000 ppm or c–f) 20 000 ppm  $\text{H}_2\text{O}$ . (a,c)  $^1\text{H}$  NMR (400 MHz) spectra showing (a) the change in  $^1\text{H}$  chemical shift and intensity of the  $\text{H}_2\text{O}$  peak from initial mixing (black line) through 24 h after mixing (red lines), (c) time-resolved emergence and consistent increase in intensity of two NH singlets at 5.74 and 6.35 ppm assigned to  $\text{d}_3$ -acetamide formation from initial mixing (black line) through 72 h after mixing (red lines). d)  $^{13}\text{C}$  NMR (126 MHz) recorded after 72 h of mixing (red lines) compared to an acetamide reference spectrum (black lines). (b,e,f) Primary mass peaks identified through HPLC-MS analysis taken 72 h after mixing with (b) 1000 ppm or (e,f) 20 000 ppm  $\text{H}_2\text{O}$  confirming the presence of (e) acetamide dimers and (f) acetamide molecules.



b) Alkaline hydrogen peroxide nitrile hydrolysis

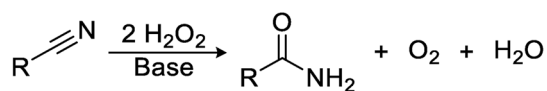


**Figure 3.** a) Interconversion of lithium peroxide and  $\text{H}_2\text{O}$  to lithium hydroperoxide and lithium hydroxide.<sup>[51]</sup> b) General scheme for nitrile hydrolysis to amides under literature-reported alkaline hydrogen peroxide conditions.<sup>[59–63]</sup>

organic chemistry. It is shown that at high discharge rates, often employed to showcase the benefits of the Li–air battery, this degradation is masked by the short discharge time, with minimal deviation from the desired  $2\text{e}^-/\text{O}_2$  ratio being observed between anhydrous cells and those doped with 1000 ppm  $\text{H}_2\text{O}$ . However, when the discharge rate is reduced, immediate deviation from the ideal  $\text{e}^-/\text{O}_2$  ratio is observed, even with meticulous drying of the cell components. This deviation is correlated to increased  $\text{H}_2\text{O}$  concentration, indicating a parasitic reaction involving  $\text{H}_2\text{O}$ . Spectroscopic characterization of a discharged



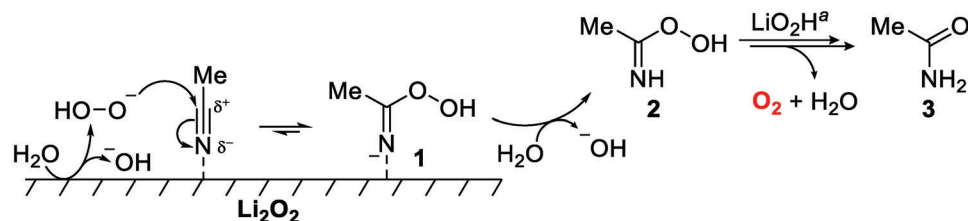


**Figure 4.** Proposed degradation pathway of MeCN by LiOOH in a hydrous Li–air system mediated by solid phase lithium peroxide. <sup>a</sup> Denotes a multistep reaction involving LiOOH, with mechanisms previously proposed in literature.<sup>[60,64,65]</sup>

electrolyte and of model chemical systems were combined to identify the degradation product as acetamide. Moreover, we propose a reaction scheme wherein solubilized LiOOH facilitates nucleophilic attack at the exposed nitrile, aided by the physical adsorption of MeCN to lithium ions on the surface of Li<sub>2</sub>O<sub>2</sub> particles or interaction with solvated Li<sup>+</sup> ions. This work highlights the possible antagonistic role of hydroperoxide species that will inevitably form in practical Li–air batteries due to atmospheric H<sub>2</sub>O. If suitable electrolyte systems are to be designed for practical Li–air batteries, the impact of hydroperoxide species and atmospheric gases must be carefully considered.

## Supporting Information

Supporting Information is available from the Wiley Online Library or from the author.

## Acknowledgements

The authors gratefully acknowledge support of this research by the Faraday Institution's Degradation and LiSTAR projects (EP/S003053/1 FITG001, FIRG014, FIRG024, FIRG051, and EP/S514901/1), the Engineering and Physical Sciences Research Council (EPSRC) New Horizon scheme (EP/V047124/1), an EPSRC Fellowship (EP/S001611/1), and the University of Nottingham's Propulsion Futures Beacon of Excellence. The authors would like to thank the University of Nottingham School of Chemistry analytical team, particularly Ben Pointer-Gleadhill for assistance with HPLC-MS method development.

## Conflict of Interest

The authors declare no conflict of interest.

## Author Contributions

All authors contributed to the conception and design of the study. R.C.M., K.D.J., and C.H. performed the experiments. All authors contributed to manuscript writing. P.G.B., D.A.W., G.N.N., H.W.L., and L.R.J. supervised the project.

## Data Availability Statement

The data that support the findings of this study are available from the corresponding author upon reasonable request.

## Keywords

acetonitrile, batteries, degradation, hydroperoxide, lithium–air batteries

Received: February 23, 2023

Revised: April 7, 2023

Published online:

- [1] T. Liu, J. P. Vivek, E. W. Zhao, J. Lei, N. Garcia-Araez, C. P. Grey, *Chem. Rev.* **2020**, *120*, 6558.
- [2] W.-J. Kwak, D. Rosy Sharon, C. Xia, H. Kim, L. R. Johnson, P. G. Bruce, L. F. Nazar, Y.-K. Sun, A. A. Frimer, M. Noked, S. A. Freunberger, D. Aurbach, *Chem. Rev.* **2020**, *120*, 6626.
- [3] J.-H. Kang, J. Lee, J.-W. Jung, J. Park, T. Jang, H.-S. Kim, J.-S. Nam, H. Lim, K. R. Yoon, W.-H. Ryu, I.-D. Kim, H. R. Byon, *ACS Nano* **2020**, *14*, 14549.
- [4] N. Imanishi, O. Yamamoto, *Mater. Today Adv.* **2019**, *4*, 100031.
- [5] D. Aurbach, B. D. McCloskey, L. F. Nazar, P. G. Bruce, *Nat. Energy* **2016**, *1*, 16128.
- [6] L. Grande, E. Paillard, J. Hassoun, J. B. Park, Y. J. Lee, Y. K. Sun, S. Passerini, B. Scrosati, *Adv. Mater.* **2015**, *27*, 784.
- [7] B. D. McCloskey, D. S. Bethune, R. M. Shelby, G. Girishkumar, A. C. Luntz, *J. Phys. Chem. Lett.* **2011**, *2*, 1161.
- [8] K. Chen, D.-Y. Yang, G. Huang, X.-B. Zhang, *Acc. Chem. Res.* **2021**, *54*, 632.
- [9] J. Lai, Y. Xing, N. Chen, L. Li, F. Wu, R. Chen, *Angew. Chem., Int. Ed.* **2020**, *59*, 2974.
- [10] R. Black, S. H. Oh, J. H. Lee, T. Yim, B. Adams, L. F. Nazar, *J. Am. Chem. Soc.* **2012**, *134*, 2902.
- [11] X. Zhang, L. Guo, L. Gan, Y. Zhang, J. Wang, L. R. Johnson, P. G. Bruce, Z. Peng, *J. Phys. Chem. Lett.* **2017**, *8*, 2334.
- [12] R. Younesi, M. Hahlin, F. Björefors, P. Johansson, K. Edström, *Chem. Mater.* **2013**, *25*, 77.
- [13] V. S. Bryantsev, M. Blanco, F. Faglioni, *J. Phys. Chem. A* **2010**, *114*, 8165.
- [14] S. Dong, S. Yang, Y. Chen, C. Kuss, G. Cui, L. R. Johnson, X. Gao, P. G. Bruce, *Joule* **2022**, *6*, 185.
- [15] N. Mahne, B. Schafzahl, C. Leypold, M. Leypold, S. Grumm, A. Leitgeb, G. A. Strohmeier, M. Wilkening, O. Fontaine, D. Kramer, C. Slugovc, S. M. Borisov, S. A. Freunberger, *Nat. Energy* **2017**, *2*, 17036.
- [16] Z. Peng, S. A. Freunberger, L. J. Hardwick, Y. Chen, V. Giordani, F. Barde, P. Novak, D. Graham, J. M. Tarascon, P. G. Bruce, *Angew. Chem., Int. Ed.* **2011**, *50*, 6351.
- [17] K. C. Lau, J. Lu, X. Luo, L. A. Curtiss, K. Amine, *ChemPlusChem* **2015**, *80*, 336.
- [18] T. Ogasawara, A. Debart, M. Holzapfel, P. Novak, P. G. Bruce, *J. Am. Chem. Soc.* **2006**, *128*, 1390.
- [19] Z. Peng, S. A. Freunberger, Y. Chen, P. G. Bruce, *Science* **2012**, *337*, 563.
- [20] M. J. Trahan, S. Mukerjee, E. J. Plichta, M. A. Hendrickson, K. M. Abraham, *J. Electrochem. Soc.* **2013**, *160*, A259.

- [21] Z. Zhang, J. Lu, R. S. Assary, P. Du, H.-H. Wang, Y.-K. Sun, Y. Qin, K. C. Lau, J. Greeley, P. C. Redfern, H. Iddir, L. A. Curtiss, *J. Phys. Chem. C* **2011**, *115*, 25535.
- [22] D. Sharon, M. Afri, M. Noked, A. Garsuch, A. A. Frimer, D. Aurbach, *J. Phys. Chem. Lett.* **2013**, *4*, 3115.
- [23] S. A. Freunberger, Y. Chen, Z. Peng, J. M. Griffin, L. J. Hardwick, F. Barde, P. Novak, P. G. Bruce, *J. Am. Chem. Soc.* **2011**, *133*, 8040.
- [24] N. Mozhzhukhina, L. P. Méndez De Leo, E. J. Calvo, *J. Phys. Chem. C* **2013**, *117*, 18375.
- [25] Y. Chen, S. A. Freunberger, Z. Peng, F. Barde, P. G. Bruce, *J. Am. Chem. Soc.* **2012**, *134*, 7952.
- [26] F. Bardé, Y. Chen, L. Johnson, S. Schaltin, J. Fransaer, P. G. Bruce, *J. Phys. Chem. C* **2014**, *118*, 18892.
- [27] D. Sharon, D. Hirsberg, M. Afri, A. Garsuch, A. A. Frimer, D. Aurbach, *J. Phys. Chem. C* **2014**, *118*, 15207.
- [28] D. Sharon, V. Etacheri, A. Garsuch, M. Afri, A. A. Frimer, D. Aurbach, *J. Phys. Chem. Lett.* **2012**, *4*, 127.
- [29] S. A. Freunberger, Y. Chen, N. E. Drewett, L. J. Hardwick, F. Barde, P. G. Bruce, *Angew. Chem., Int. Ed.* **2011**, *50*, 8609.
- [30] X. Gao, Y. Chen, L. R. Johnson, Z. P. Jovanov, P. G. Bruce, *Nat. Energy* **2017**, *2*, 17118.
- [31] B. D. Adams, R. Black, Z. Williams, R. Fernandes, M. Cuisinier, E. J. Berg, P. Novak, G. K. Murphy, L. F. Nazar, *Adv. Energy Mater.* **2015**, *5*, 1400867.
- [32] R. Younesi, P. Norby, T. Vegge, *ECS Electrochem. Lett.* **2014**, *3*, A15.
- [33] A. Khetan, A. Luntz, V. Viswanathan, *J. Phys. Chem. Lett.* **2015**, *6*, 1254.
- [34] V. S. Bryantsev, V. Giordani, W. Walker, M. Blanco, S. Zecevic, K. Sasaki, J. Uddin, D. Addison, G. V. Chase, *J. Phys. Chem. A* **2011**, *115*, 12399.
- [35] C. O. Laoire, S. Mukerjee, K. M. Abraham, E. J. Plichta, M. A. Hendrickson, *J. Phys. Chem. C* **2010**, *114*, 9178.
- [36] M. Mwemezi, S. J. R. Prabakar, S. C. Han, J. Y. Seo, W. B. Park, J.-W. Lee, K.-S. Sohn, M. Pyo, *J. Mater. Chem. A* **2021**, *9*, 4962.
- [37] D. Farhat, J. Maibach, H. Eriksson, K. Edström, D. Lemordant, F. Ghamouss, *Electrochim. Acta* **2018**, *281*, 299.
- [38] V. S. Bryantsev, J. Uddin, V. Giordani, W. Walker, D. Addison, G. V. Chase, *J. Electrochem. Soc.* **2013**, *160*, A160.
- [39] C. L. Yaws, M. A. Satyro, in *The Yaws Handbook of Vapor Pressure*, 2nd ed. (Ed.: C. L. Yaws), Gulf Professional Publishing, Houston, Texas **2015**, pp. 1–314.
- [40] X. Gao, Y. Chen, L. Johnson, P. G. Bruce, *Nat. Mater.* **2016**, *15*, 882.
- [41] J. M. Cameron, C. Holc, A. J. Kibler, C. L. Peake, D. A. Walsh, G. N. Newton, L. R. Johnson, *Chem. Soc. Rev.* **2021**, *50*, 5863.
- [42] J. Wang, J. Zheng, X. Liu, *Phys. Chem. Chem. Phys.* **2022**, *24*, 17920.
- [43] Y. Hase, Y. Komori, T. Kusumoto, T. Harada, J. Seki, T. Shiga, K. Kamiya, S. Nakanishi, *Nat. Commun.* **2019**, *10*, 596.
- [44] Y. Hase, K. Nishioka, Y. Komori, T. Kusumoto, J. Seki, K. Kamiya, S. Nakanishi, *J. Phys. Chem. Lett.* **2020**, *11*, 7657.
- [45] B. D. McCloskey, D. S. Bethune, R. M. Shelby, T. Mori, R. Scheffler, A. Speidel, M. Sherwood, A. C. Luntz, *J. Phys. Chem. Lett.* **2012**, *3*, 3043.
- [46] B. D. McCloskey, C. M. Burke, J. E. Nichols, S. E. Renfrew, *Chem. Commun.* **2015**, *51*, 12701.
- [47] K. G. Gallagher, S. Goebel, T. Greszler, M. Mathias, W. Oelerich, D. Eroglu, V. Srinivasan, *Energy Environ. Sci.* **2014**, *7*, 1555.
- [48] D. G. Kwabi, T. P. Batcho, S. Feng, L. Giordano, C. V. Thompson, Y. Shao-Horn, *Phys. Chem. Chem. Phys.* **2016**, *18*, 24944.
- [49] Y. Qiao, S. Wu, J. Yi, Y. Sun, S. Guo, S. Yang, P. He, H. Zhou, *Angew. Chem., Int. Ed.* **2017**, *56*, 4960.
- [50] S. Meini, M. Piana, N. Tsiouvaras, A. Garsuch, H. A. Gasteiger, *Electrochem. Solid-State Lett.* **2012**, *15*, A45.
- [51] H. A. Gasteiger, M. Piana, T. Restle, M. Metzger, K. U. Schwenke, *J. Electrochem. Soc.* **2015**, *162*, A573.
- [52] J. M. García, L. E. Krupp, V. Viswanathan, B. D. McCloskey, A. C. Luntz, N. B. Aetukuri, *Nat. Chem.* **2014**, *7*, 50.
- [53] A. E. Torres, P. B. Balbuena, *Chem. Mater.* **2018**, *30*, 708.
- [54] F. Li, S. Wu, D. Li, T. Zhang, P. He, A. Yamada, H. Zhou, *Nat. Commun.* **2015**, *6*, 7843.
- [55] T. Liu, Z. Liu, G. Kim, J. T. Frith, N. Garcia-Araez, C. P. Grey, *Angew. Chem., Int. Ed.* **2017**, *56*, 16057.
- [56] M. Berholts, H. Myllynen, K. Kooser, E. Itälä, S. Granroth, H. Levola, J. Laksman, S. Oghbaiee, B. Oostenrijk, E. Nömmiste, E. Kukk, *J. Chem. Phys.* **2017**, *147*, 194302.
- [57] V. K. C. Chau, Z. Chen, H. Hu, K.-Y. Chan, *J. Electrochem. Soc.* **2017**, *164*, A284.
- [58] T. Laino, A. Curioni, *New J. Phys.* **2013**, *15*, 095009.
- [59] G. W. Kabalka, S. M. Deshpande, P. P. Wadgaonkar, N. Chatla, *Synth. Commun.* **1990**, *20*, 1445.
- [60] G. D. Yadav, J. L. Ceasar, *Org. Process Res. Dev.* **2008**, *12*, 740.
- [61] D. P. Canterbury, F. Godin, S. Desjardins, M. Bayraktarian, J. S. Albert, D. A. Perry, K. D. Hesp, *Org. Lett.* **2018**, *20*, 5336.
- [62] A. R. Katritzky, B. Pilarski, L. Urogdi, *Synthesis* **1989**, 1989, 949.
- [63] W. Zhan, L. Ji, Z. Ge, X. Wang, R. Li, *Tetrahedron* **2018**, *74*, 1527.
- [64] K. B. Wiberg, *J. Am. Chem. Soc.* **1953**, *75*, 3961.
- [65] J. E. McIsaac, R. E. Ball, E. J. Behrman, *J. Org. Chem.* **1971**, *36*, 3048.
- [66] T. K. Zakharchenko, A. I. Belova, A. S. Frolov, O. O. Kapitanova, J.-J. Velasco-Velez, A. Knop-Gericke, D. Vyalikh, D. M. Itkis, L. V. Yashina, *Top. Catal.* **2018**, *61*, 2114.